Combination of Gravimetry, Altimetry and GOCE Data for Geoid Determination in the Mediterranean: Evaluation by Simulation

R. Barzaghi [(1)], A. Maggi [(1)], N. Tselfes [(2)], D. Tsoulis [(3)], I. N. Tziavos [(3)], G. S. Vergos [(3)]

[(1)] DIIAR - Politecnico di Milano - Piazza Leonardo da Vinci, 32 - 20133 Milano - Italy
[(2)] DIIAR - Politecnico di Milano, Polo Regionale di Como - Via Valleggio, 11 - 22100 Como - Italy
[(3)] Department of Geodesy and Surveying, Aristotle University of Thessaloniki, University Box440, 54124 Thessaloniki - Greece

Abstract. Local geoid determination is traditionally carried out on land and at sea areas using gravity anomaly and altimetry data. This determination can be aided and improved by the data of missions such as GOCE. In order to assess the performance of the combination of heterogeneous data for local geoid determination, simulated data for the area of the central Mediterranean Sea are analyzed. These data include gravity anomaly, altimetry, and GOCE observations processed with the space-wise approach.

The results show that GOCE data improve the results for areas not well covered with other data types, while also accounting for any long wavelength errors of the adopted reference model. Even when the ground gravity data are dense, data from GOCE improve the error standard deviation and eliminate biases.

At sea, the altimetry data give the dominant geoid information. However the geoid accuracy is sensitive to orbit calibration errors and the unmodelled mean sea surface topography. If such effects are present the GOCE data can account for them.

Keywords. Mediterranean geoid, GOCE mission, gravity, altimetry.

1 Introduction

GOCE (Gravity field and steady-state Ocean Circulation Explorer) is a satellite mission (ESA, 1999) designed by ESA (European Space Agency), which will be launched in 2008. The goal of this mission is the determination of the stationary part of the gravity field to a high degree of accuracy and spatial resolution. The main instrument on board the satellite will be the "gradiometer", composed by six accelerometers, and measuring the second derivatives of the potential (the full tensor) along the satellite orbit (the so-called gradients). Additional information on the gravity field will be derived from the tracking of the satellite orbit, by means of a GPS receiver, and the accelerometers measurements of the non-gravitational forces..

Three different approaches will be applied for the determination of the global gravity field models from GOCE: the direct approach (Bruinsma et al., 2004), the time-wise approach (Pail et al., 2005) and the space-wise approach (Migliaccio et al., 2004).

In a previous study (Maggi et al, 2007), the contribution of GOCE filtered data from the space-wise approach and a GOCE geo-potential model, were evaluated for local geoid determination in a combination scheme with terrestrial data employing least squares collocation in a simulation. It was found that the benefit from the GOCE long wave-length information will be very significant. The present paper, refers to a larger region incorporating satellite altimetry data as well. No topographic information (Arabelos and Tscherning, 1990) or bathymetric information (Vergos and Sideris, 2003) will be used for data reduction, even though this is possible with real data.

2 Simulation of data

In the frame of the EGG-C (European GOCE Gravity Consortium) (Balmino, 2001) activities for the preparation of the GOCE mission, full simulation solutions are computed so that methodology and software efficiency are ensured (Migliaccio et al., 2006). The latest simulated data set available by EGG-C is used and the data are processed. These data include 60 days (note that at least 1 year is expected) of: gradients with in-flight calibration noise (including instrumental errors, satellite errors, etc.), signal simulated from EGM96 (Lemoine et al, 1998), orbit positions and velocities, common mode accelerations, rotations and attitude information. The orbit positions and velocities are used to obtain

(pseudo-) observations of the disturbing potential along the orbit (Jekeli, 1999). These data are processed with the space-wise approach. This is a multi-step collocation procedure that consists of the Wiener filter, gridding by least squares collocation, harmonic analysis of the grids, and iterations made in order to account for the non-optimality of the Wiener filter. For details of these steps and related results with these data, see (Migliaccio et al, 2007). For the present study a filtered grid of potential T and a grid of second order radial derivatives T_{rr} are used. In the latitude interval -83 to 83 degrees these grids have an error Standard Deviation (STD) of 0.022 m^2s^{-2} and 0.61 $10^{-12}s^{-2}$ (milli-Eötvös) respectively. The high quality of the T grid is also due to noise-free positions used. The accuracy is much smaller over the poles because of the GOCE orbit inclination (i = 96.5°). Note that the gradients are measured in the gradiometer reference frame (x,y,z) but through the filtering and gridding they are transformed into the Local Orbital Reference Frame (ξ,η,r) (LORF), where ξ is almost along-track, η cross-track and r radial.

Ground gravity anomalies Δg are simulated with the signal from EGM96 up to degree and order 360 and white noise of 5 mgal. A set of true available observations is used for the longitude and latitude. The EGM96 reference sphere is used as radius.

The altimetry simulation is based on the data from the Geodetic Mission (phase E) of ERS1 as provided by AVISO (1998) in the merged T/P & ERS1 corrected Sea Surface Heights (CORSSHs) products. This set of ERS1 SSHs refers to reprocessed data which have improved orbit accuracy. The procedure followed was based on fitting the original ERS data (NOAA JGM-2 orbits) to the more precise TOPEX/Poseidon data (JGM-3 orbits) using a global minimization principle of the ERS1-T/P dual crossover differences (Le Traon et al., 1995; Le Traon and Ogor, 1998). Based on this adjustment, improved ERS orbits with an accuracy similar to T/P ones (2cm rms) was obtained. Observations of the geoid N are generated from EGM96. A generous error is added to them: track-wise bias and tilt, plus white noise of total 4cm RMS (Root of Mean Square). A "bow tie" error (Schrama, 1989) of 3.5cm RMS is also simulated, but it is not added unless specified so.

In order to have a more detailed geoid in the simulation, the GPM98 model (Wenzel, 1998) is added to all the data, from degree 361 to 720 and order 0 to 720. For the collocation solution, EIGEN_gl04c (Förste et al, 2007) is subtracted, up to degree and order 360, from all the data (Fig. 1). The differences of this model to EGM96 are interpreted as long wave-length errors. This does not imply a judgement by the authors about the quality of these models. These differences are similar to the nominal EGM96 errors (Maggi et al, 2007) and this is useful to perform simulations where a model with long wavelength errors is used as reference.

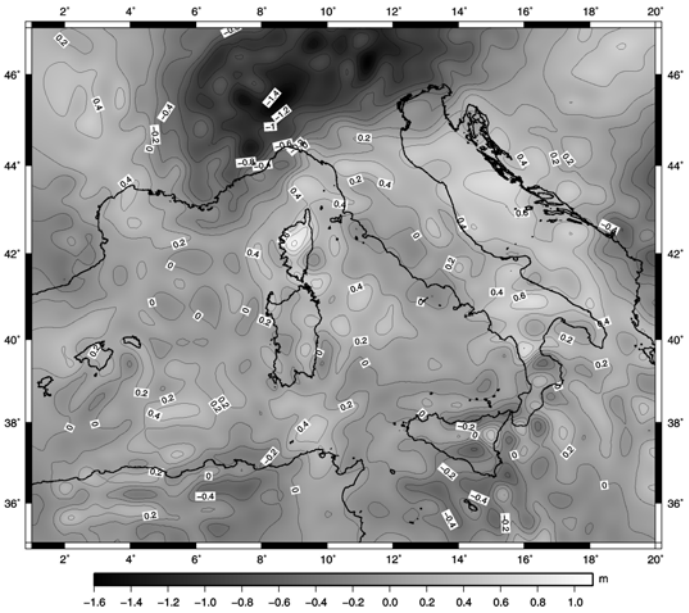

Fig. 1 The simulated geoid of the central Mediterranean, i.e. the synthesis from EGM96 and GPM98 referenced to EIGEN_gl04c.

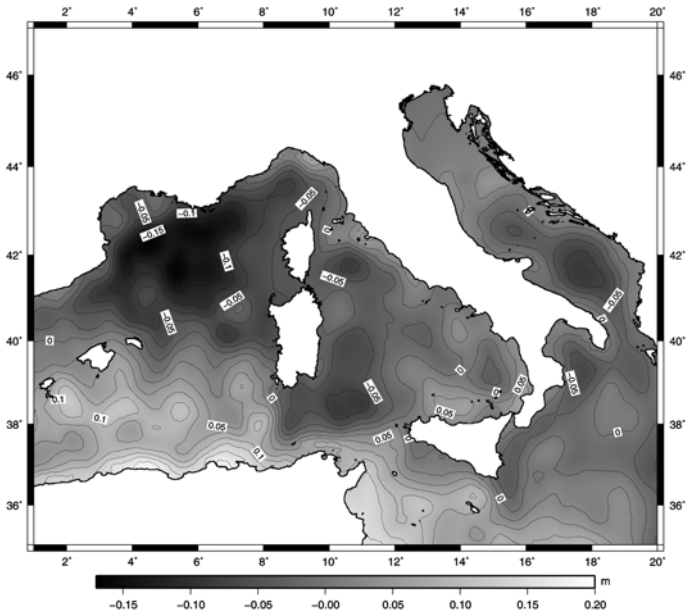

Fig. 2 The simulated MDSST.

A Mean Dynamic Sea Surface Topography (MDSST) is also simulated. The model determined by Rio (2004) (Fig. 2) is taken and interpolated to the altimetry points. The MDSST is not present in the altimetry observations, unless specified so.

3 Local geoid determination

3.1 Collocation with ground gravity and altimetry data

A local geoid determination is often made using the well-known method of least squares collocation (Moritz, 1980).
The predicted geoid undulation based on gravity and undulation is given by:

$$\hat{\mathbf{N}} = \mathbf{C}_{Ns}\left(\mathbf{C}_{ss} + \mathbf{C}_{vv}\right)^{-1}\mathbf{y}\,, \tag{1}$$

where $\mathbf{y}$ is the vector of observed Δg and N, $\mathbf{C}_{ss}$ is a matrix computed from the Δg and N covariances and cross-covariances, $\mathbf{C}_{Ns}$ is a matrix computed from the cross-covariances of the predicted N with the observed Δg and N and $\mathbf{C}_{vv}$ describes the Δg and N noise. In spherical approximation, the covariance and cross-covariance functions to be used in (1) are obtained by:

$$C_{\Delta g_P,\Delta g_Q} = \frac{\mu^2}{R^4}\sum_{\ell=\ell_{\min}}^{\ell_{\max}} {\alpha_\ell}^2\tilde{\sigma}_\ell^2\left(\frac{R^2}{r_P r_Q}\right)^{\ell+2} P_\ell(t), \tag{2}$$

$$C_{\Delta g_P,N_Q} = \frac{1}{\bar{\gamma}}C_{\Delta g_P,T_Q}\,, \tag{3}$$

$$C_{\Delta g_P,T_Q} = \frac{\mu^2}{R^3}\sum_{\ell=\ell_{\min}}^{\ell_{\max}} \alpha_\ell\tilde{\sigma}_\ell^2\left(\frac{R}{r_P}\right)^{\ell+2}\left(\frac{R}{r_Q}\right)^{\ell+1} P_\ell(t), \tag{4}$$

$$C_{N_P,N_Q} = \frac{1}{\bar{\gamma}^2}C_{T_P,T_Q}\,, \tag{5}$$

$$C_{T_P,N_Q} = \frac{1}{\bar{\gamma}}C_{T_P,T_Q}\,, \tag{6}$$

$$C_{T_P,T_Q} = \frac{\mu^2}{R^2}\sum_{\ell=\ell_{\min}}^{\ell_{\max}} \tilde{\sigma}_\ell^2\left(\frac{R^2}{r_P r_Q}\right)^{\ell+1} P_\ell(t), \tag{7}$$

where $t=\cos(\psi)$, ψ is the spherical distance, $P_\ell(t)$ are Legendre polynomials of degree ℓ, R is the mean earth radius, r_P, r_Q are the radii of points P and Q, μ is the gravitational constant times the

earth mass, $\tilde{\sigma}_\ell^2$ are some adapted signal degree variances and $a_\ell = (\ell - 1)$.

The quantity $\bar{\gamma}$ is the mean normal gravity used throughout the simulations.

The prediction error covariance matrix is computed by (Moritz, 1980):

$$\mathbf{C}_e = \left(\mathbf{C}_{NN} - \mathbf{C}_{sN}^T \left(\mathbf{C}_{ss} + \mathbf{C}_{vv}\right)^{-1} \mathbf{C}_{sN}\right), \quad (8)$$

where, the matrix $\mathbf{C}_{NN}$ is computed from the N covariance function. For comparisons with the actual errors computed from simulations, the point-wise STD is used:

$$\sigma_i = \sqrt{\mathbf{C}_e(i,i)}\,. \quad (9)$$

3.2 Utilization of GOCE data

The functions (eq. 4), (eq. 6) and (eq. 7) are those suitable for including gridded potential in the geoid prediction. For the gridded second radial derivatives, the following functions are also needed: the covariance function of T_{rr} and its cross covariance functions with T, Δg and N.

$$C_{T_{rrP},T_{rrQ}} = \frac{\mu^2}{R^6} \sum_{\ell=\ell_{\min}}^{\ell_{\max}} \beta_\ell{}^2 \tilde{\sigma}_\ell^2 \left(\frac{R^2}{r_P r_Q}\right)^{\ell+3} P_\ell(t), \quad (10)$$

$$C_{T_{rrP},T_Q} = \frac{\mu^2}{R^4} \sum_{\ell=\ell_{\min}}^{\ell_{\max}} \beta_\ell\, \tilde{\sigma}_\ell^2 \left(\frac{R}{r_P}\right)^{\ell+3} \left(\frac{R}{r_Q}\right)^{\ell+1} P_\ell(t), \quad (11)$$

$$C_{\Delta g_P,T_{rrQ}} = \frac{\mu^2}{R^5} \sum_{\ell=\ell_{\min}}^{\ell_{\max}} \delta_\ell\, \tilde{\sigma}_\ell^2 \left(\frac{R}{r_P}\right)^{\ell+2} \left(\frac{R}{r_Q}\right)^{\ell+3} P_\ell(t), \quad (12)$$

$$C_{T_{rrP},N_Q} = \frac{1}{\bar{\gamma}} C_{T_{rrP},T_Q}\,, \quad (13)$$

where, $\beta_\ell = (\ell+1)(\ell+2)$ and $\delta_\ell = \alpha_\ell \beta_\ell$.

The covariance functions needed for T_{rr} are easy to compute because the radial direction of LORF coincides with the up direction of an East-North-Up (ENU) frame. If other derivatives along directions not coinciding with ENU were to be used then all the covariance functions would have to be computed and linear combinations would have to be made, according to the rotations between the used directions and the ENU (Tscherning, 1993). This procedure is made inside the space-wise approach, because the other two directions of LORF differ from the East and North. However the gridded second radial derivatives produced with the space-wise approach are easy to handle in collocation.

If all four data types are used, vector $\mathbf{y}$ (Eq. 1) now includes, in addition to Δg and N, the gridded T and T_{rr}. The signal and error matrices (Eqs. 4 and 8) include the covariances of T_{rr} and T and their cross covariances with Δg and N.

3.3 A simulation of geoid prediction

The simulated geoid over the central Mediterranean is examined. The considered area is bounded between $35^o<\varphi<47^o$ and $2^o<\lambda<20^o$ and divided in 24 cells of 3 by 3 degrees. The geoid is predicted by least squares collocation on a regular spherical grid of 0.2 degrees. A separate collocation is made for every cell. A limit for the number of data is set: 1500 gravity anomalies Δg per cell / 2000 for 3 cells that cover the Alps, 1500 altimetry observations N per cell, 1100 gridded T_{rr} and 350 gridded T. Δg and N are taken with overlap of 1^o around each cell, while GOCE gridded data are taken with 2^o overlap.

The degree variances $\tilde{\sigma}_\ell^2$ are based on considering a-priori knowledge of the degree variances of the differences between EGM96 and EIGEN_gl04c, up to degree 360, and the signal degree variances of GMP98 from degree 361 to 720. These degree variances are scaled to fit the gravity anomaly variance locally. Consistency between the true errors and the predicted errors (Eq. 9) justify this simple choice. For optimal results a simultaneous fit to T_{rr} and Δg could be made (Knudsen, 1987) and for real data closed covariance expressions up to infinite degree (Tscherning and Rapp, 1974) can be used. A more thorough study about the degree variances estimation for the combination of heterogeneous data types is a very interesting and important topic on its own, though it is this is not addressed here. Fortunately the collocation results are robust to some variations of the covariance function (Sansò et al., 1999).

For the 24 cells of the whole area the addition of GOCE data to the already available Δg and N data leads to significant improvement (Table 1). Edge effects, data gaps and distribution problems are resolved with GOCE.

The effect of heterogeneous data combination is better seen if smaller areas are examined. Therefore, four “zoom-in” cases, from the twenty four examined, are presented herein. All refer to areas included in a single 3 by 3 cell, so that no errors of cells treated separately are mixed.

Table 1. Geoid prediction errors, in cm, for the whole area (case whole.) and different data combinations.

case	data used	STD	RMS
whole.	Δg	16.5	17.1
whole.	Δg, N	9.9	9.9
whole.	Δg, N, T_{rr}	5.1	5.0
whole.	Δg, N, T, T_{rr}	4.8	4.8

The first zoom is made in the area between $44^o<\varphi<47^o$ and $6^o<\lambda<8^o$. This is inside a cell with 2000 Δg that covers mostly the Alps. It is seen that GOCE improves the error STD but improves much more the RMS (Table 2) because the Δg only solution has a mean value problem. This problem is present in almost all the cells, regardless of the number and distribution of Δg. The solution for this cell is repeated with 1000 points of Δg and 650 points of T_{rr}. It is seen that is better to add some GOCE data than to increase the number of Δg observations.

The second "zoom" is made in an area between $42^o<\varphi<44^o$ and $11^o<\lambda<13^o$. There, the mean value problem solution with the use of T is seen (Table 3).

Table 2. Geoid prediction errors, in cm, for an area in the Alps for 2000 Δg, 1100 T_{rr} and 350 T (case alps 1.) and for 1000 Δg and 650 T_{rr} (alps 2) for different data combinations.

case	data used	STD	RMS
alps 1.	Δg	9.7	15.2
alps 1.	Δg, T_{rr}	4.8	5.1
alps 1.	Δg, T, T_{rr}	4.7	4.7
alps 2.	Δg,	6.1	6.1

Table 3. Geoid prediction errors, in cm, for an area in central Italy for 1500 Δg and 350 T (case centre 1).

case	data used	STD	RMS
centre 1.	Δg	5.4	12.9
centre 1.	Δg, T	3.1	3.1

The third "zoom" is made at a cell bounded between $41^o<\varphi<43^o$ and $5^o<\lambda<8^o$ degrees. The dense altimetry data give a very good solution (Table 4). If the MDSST is added this quality is degraded. This effect is present at every area where the MDSST is high. If GOCE data are added most of these problems are fixed. From the fourth "zoom", referring to the area between $35^o<\varphi<38^o$ and $17^o<\lambda<20^o$ degrees, a similar result is obtained. When the bow tie error is added to altimetry data, long wave-length errors arise, but they are corrected significantly when GOCE data are added (Table 5). An important conclusion can be drawn based on the aforementioned results, i.e., that the altimetric information dominates, but unmodelled MDSST and possible "bow tie" errors can be identified and consequently corrected with the information of GOCE.

A final test for a large area between $35^o<\varphi<47^o$ and $0^o<\lambda<20^o$ is performed. 6000 Δg are used, distributed on a grid and with a 3 mgal white noise, thus simulating an interpolated grid. The estimate was predicted at 2145 stations in the area $37^o<\varphi<45^o$ and $2^o<\lambda<18^o$. Then, the impact of using 6000 of the gridded T or T_{rr} values, distributed on the same grid used for Δg, is tested. The decisive contribution of these data when combined with gravity anomalies is verified, even for a large area with good distribution of Δg and with lower noise (table 6).

Table 4. Geoid prediction errors, in cm, for an area of sea, (case sea 1.) and the same area but with altimetry observations containing the MDSST (case sea 2).

case	data used	STD	RMS
sea 1.	N	1.5	1.5
sea 2.	N	3.4	12.4
sea 2.	N, T, T_{rr}	3.7	3.8
sea 2.	N, Δg, T, T_{rr}	3.0	3.0

Table 5. Geoid prediction errors, in cm, for an area of sea, (case sea 1.) and the same area but with altimetry observations with "bow tie" error (case sea 2).

case	data used	STD	RMS
sea 1.	N	1.6	1.7
sea 2.	N	2.7	8.8
sea 2.	N, T, T_{rr}	3.3	3.5
sea 2.	N, Δg, T, T_{rr}	2.8	3.0

Table 6. Geoid prediction errors, in cm, for a large test area with 6000 Δg, T_{rr} and T (case large).

case	Data used	STD	RMS
large.	Δg	7.0	8.0
large.	T_{rr}	13.5	13.5
large.	T	15.1	15.1
large.	Δg, T_{rr}	3.8	3.8
large.	Δg, T	3.6	3.6

4 Conclusions

Both, the GOCE data and the gravity field model derived from GOCE data, are expected to present good long wavelength information. This will be very useful for local gravity field modelling. The results presented in this paper show that the use of processed GOCE data significantly increases the accuracy of local geoid estimation with gravity data on ground or at sea and the use of GOCE potential estimates resolves mean value problems.

In marine regions the altimetric information dominates and spans the entire geoid spectrum. However if MDSST effects and/or errors like the "bow tie" exist, other long wave-length information, just like that of GOCE, is needed. The latter points out the utility of GOCE for MDSST estimation, as well as the possible use of GOCE data for calibration of other data types.

Acknowledgements

This work was performed under ESA contract No. 18308/04/NL/NM (GOCE HPF) and in the frame of the 3rd Community Support Program (Opp. Supp. Progr. 2000 - 2006), Measure 4.3, Action 4.3.6, Sub-Action 4.3.6.1 (International Scientific and Technological Co-operation), bilateral cooperation between Greece and Italy.

References

Arabelos, D. and C. C. Tscherning (1990). Simulation of regional gravity field recovery from satellite gradiometer data using collocation and FFT. *Bulletin Geodesique.* 64, pp. 363-382.

AVISO (1998) AVISO User Handbook – Corrected Sea Surface Heights (CORSSHs), AVI-NT-011-311-CN, Ed 3.1.

Balmino, G. (2001). The European GOCE Gravity Consortium (EGG-C). In: *Proc. of 1st International GOCE User Workshop.* ESA-ESTEC, Noordwijk, The Netherlands, April 23-24 2001.

Bruinsma, S., J.C. Marty and G. Balmino (2004). Numerical simulation of the gravity field recovery from GOCE mission data. In: *Proc. of 2nd International GOCE User Workshop.* Frascati, Italy, March 8-10 2004.

ESA (1999). Gravity Field and Steady-State Ocean Circulation Mission. ESA SP-1233 (1). ESA Publication Division, c/o ESTEC, Noordwijk, The Netherlands.

Förste Ch., F. Flechtner, R. Schmidt, R. König, U. Meyer, R. Stubenvoll, M. Rothacher, F. Barthelmes, H. Neumayer, R. Biancale, S. Bruinsma, J. M. Lemoine, S. Loyer (2007). Global mean gravity field models from combination of satellite mission and altimetry / gravimetry surface data. *Proc. of the 3rd international GOCE user workshop*, 6-8 November 2006, Frascati, Italy.

Jekeli, C. (1999). The determination of gravitational potential differences from satellite-to-satellite tracking. *Celestial Mechanics and Dynamical Astronomy*, 75, pp. 85-101.

Knudsen, P. (1987). Estimation and modelling of the local empirical covariance function using gravity and satellite altimeter data. *Bulletin Geodesique.* 61, pp. 145-160.

Le Traon PY, Ogor F (1998) ERS-1/2 orbit improvement using Topex/Poséidon: The 2 cm challenge. *J Geophys Res*(103)C4: 8045-8057.

Le Traon PY, Gaspar P, Bouyssel F, Makhmara H (1995) Using TOPEX/POSEIDON data to enhance ERS-1 orbit. J Atm Ocean Tech 12: 161-170.

Lemoine, F.G., S.C. Kenyon, J.K. Factor, R.G. Trimmer, N.K. Pavlis, D.S. Chinn, C.M. Cox, S.M. Klosko, S.B. Luthcke, M.H. Torrence, Y.M. Wang, R.G. Williamson, E.C. Pavlis, R.H. Rapp and T.R. Olson (1998). The development of the joint NASA GSFC and NIMA geopotential model EGM96. NASA/TP-1998-206861, Goddard Space Flight Center, Greenbelt, Maryland.

Maggi A., F. Migliaccio, M. Reguzzoni and N. Tselfes (2007). Combination of Ground Gravimetry and GOCE Data for Local Geoid Determination: a Simulation Study. Proc. of the 1st International Symposium of the International Gravity Field Service, August 28 - September 01, 2006, Istanbul, Turkey, In print.

Migliaccio, F., M. Reguzzoni, and F. Sansò (2004). Space-wise approach to satellite gravity field determination in the presence of coloured noise. *Journal of Geodesy*, 78, pp. 304-313.

Migliaccio, F., M. Reguzzoni, and N. Tselfes (2006). GOCE: a full-gradient Solution in the Space-wise Approach. *Proc. Of the IAG2005 – Scientific Assembly*, 22-26 August 2005, Cairns, Australia. P. Tregoning and C. Rizos (eds), Vol. 130, Springer, Berlin, pp. 383-390.

Migliaccio, F., M. Reguzzoni M, Sansò F., Tselfes N., Tscherning C. C., Veicherts M. (2007). The latest of the space-wise approach for GOCE data analysis. *Proc. of the 3rd international GOCE user workshop*, 6-8 November 2006, Frascati, Italy.

Moritz, H. (1980). Advanced Physical Geodesy. Wichmann, Karlsruhe.

Pail, R., W.D. Schuh and M. Wermuth (2005). GOCE Gravity Field Processing. In: *International Association of Geodesy Symposia, 'Gravity, Geoid and Space Missions'*, C. Jekeli, L. Bastos and J. Fernandes (eds), vol. 129, Springer-Verlag, Berlin, pp. 36-41.

Rio M.-H. (2004) A Mean Dynamic Topography of the Mediterranean Sea Estimated from the Combined use of Altimetry, In-Situ Measurements and a General Circulation Model. Geoph Res Let Vol. 6, 03626.

Sansò, F., G. Venuti and C. C. Tscherning (1999). A theorem of insensitivity of the collocation solution to variations of the metric of the interpolation space. *In: International Association of Geodesy Symposia*, vol. 121, K.P. Schwarz ed., Springer-Verlag, Berlin, pag. 233-240.

Schrama, E. J. O. (1989): The Role of Orbit Errors in Processing of Satellite Altimeter Data. Report No. 33, *Netherlands Geodetic Commision. Publications on geodesy, New series.* Delft, 1989.

Tscherning, C. C. (1993). Computation of Covariances of Derivatives of the Anomalous Gravity Potential in a Rotated Reference Frame. *Manuscripta Geodaetica*, 18, pp. 115-123.

Tscherning, C.C. and R.H. Rapp (1974): Closed Covariance Expressions for Gravity Anomalies, Geoid Undulations, and Deflections of the Vertical Implied by Anomaly Degree-Variance Models. *Reports of the Department of Geodetic Science* No. 208, The Ohio State University, Columbus, Ohio.

Vergos, G.S. and M.G. Sideris (2003): Altimetry-Derived Marine Gravity Field Estimation from Multi-Satellite Data. *Proc. Of the 3rd Meeting of the International Gravity and Geoid Commission,* August 26-30, 2002, Thessaloniki, Greece, I.N. Tziavos (ed), Ziti editions, pp 314-319.

Wenzel, G. (1998). Ultra high degree geopotential models GPM98A, B and C to degree 1800. *Proceedings Joint Meeting of the International Gravity Commission and International Geoid Commission*, September 7-12, Trieste 1998. Bollettino di Geofisica teorica ed applicata.